Local non-similarity solutions for the flow of a non-Newtonian fluid over a wedge

Mehrdad Massoudi*

U.S. Department of Energy, National Energy Technology Laboratory, P.O. Box 19040, Pittsburgh, PA 15236, USA

Received 7 January 2000; accepted 15 June 2000

Abstract

The boundary layer and heat transfer equations for a non-Newtonian fluid, represented by a power-law model, over a porous wedge is studied. The free stream velocity, the surface temperature variations, and the injection velocity at the surface are assumed variables. Similar and non-similar solutions are presented and the restrictions for these cases are studied. The results are presented for velocity and temperature profiles for various values of the dimensionless numbers. The effects of the different parameters on the skin friction co-efficient and the local heat transfer co-efficient are also studied. Published by Elsevier Science Ltd.

Keywords: Power-law model; Non-Newtonian fluid; Similar and non-similar solutions; Drag reduction; Fluids of differential type

1. Introduction

Mechanics of non-linear fluids present a special challenge to engineers, physicists, and mathematicians. The non-linearity can manifest itself in a variety of ways. One of the simplest ways in which the viscoelastic fluids have been classified is the methodology given by Rivlin and Ericksen [1] and Truesdell and Noll [2], who present constitutive relations for the stress tensor **T** as a function of the symmetric part of the velocity gradient **D**, and its higher (total) derivatives. (Another class of models is the rate-type fluid models, such as Oldroyd [3] model. A recent review is given by Rajagopal and Srinivasa [4]). Fluids of differential type have attracted much attention, as well as much controversy, in the last few decades. We refer the reader to Dunn and Rajagopal [5] for a complete and thorough discussion of all the relevant issues. The major attractiveness of these models is the fact that the constitutive relations, whether we take the second- or the third-grade fluids since they have been studied the most, are that they are derived based on first principles and unlike many other 'phenomenological' models (cf. Reiner [6]), there are no curve-fittings or parameters to adjust. Though, in both of these grade models, there are material properties that need to be measured. At the same time, the 'sign' of these material parameters and the stability or instability of the motions have caused a certain degree of misunderstanding. These issues for the second- and third-grade fluids have been discussed in detail by Dunn and Fosdick [7], and Fosdick and Rajagopal [8], respectively.

* Tel.: + 1-412-386-4975; fax: + 1-412-386-4806.
E-mail address: massoudi@netl.doe.gov (M. Massoudi).

The stress in a third grade fluid is given by [2]

$$\mathbf{T} = -p\mathbf{1} + \mu\mathbf{A}_1 + \alpha_1\mathbf{A}_2 + \alpha_2\mathbf{A}_1^2 + \beta_1\mathbf{A}_3 + \beta_2\{\mathbf{A}_1\mathbf{A}_2 + \mathbf{A}_2\mathbf{A}_1\} + \beta_3(\mathrm{tr}\,\mathbf{A}_1^2)\mathbf{A}_1, \tag{1}$$

where μ is the coefficient of viscosity, and α_1, α_2, β_1, β_2, and β_3 are the material moduli. In the above representation, $-p\mathbf{1}$ is the spherical stress due to the constraint of incompressibility, and the kinematical tensors $\mathbf{A}_1$, $\mathbf{A}_2$, and $\mathbf{A}_3$ are defined by

$$\mathbf{A}_1 = (\mathrm{grad}\,\mathbf{v}) + (\mathrm{grad}\,\mathbf{v})^{\mathrm{T}}, \tag{2}$$

$$\mathbf{A}_n = \frac{\mathrm{d}}{\mathrm{d}t}\mathbf{A}_{n-1} + \mathbf{A}_{n-1}(\mathrm{grad}\,\mathbf{v}) + (\mathrm{grad}\,\mathbf{v})^{\mathrm{T}}\mathbf{A}_{n-1},$$

$$n = 2, 3, \tag{3}$$

when $\mathbf{v}$ denotes the velocity field, grad is the gradient operator, and $\mathrm{d}/\mathrm{d}t$ is the material time derivative, which is defined by

$$\frac{\mathrm{d}(\cdot)}{\mathrm{d}t} = \frac{\partial(\cdot)}{\partial t} + [\mathrm{grad}(\cdot)]\mathbf{v}, \tag{4}$$

where $\partial/\partial t$ is the partial derivative with respect to time. A detailed thermodynamic analysis of the model, represented by Eq. (1) is given by Fosdick and Rajagopal [8]. They showed that if all the motions of the fluid are to be compatible with thermodynamics in the sense that these motions meet the Clausius–Duhem inequality and if it is assumed that the specific Helmholtz free energy is a minimum when the fluid is locally at rest, then

$$\mu \geqslant 0, \quad \alpha_1 \geqslant 0,$$

$$|\alpha_1 + \alpha_2| \leqslant \sqrt{24\mu\beta_3},$$

$$\beta_1 = \beta_2 = 0, \quad \beta_3 \geqslant 0. \tag{5}$$

Therefore, the constitutive relation for a thermodynamically compatible fluid of grade three becomes

$$\mathbf{T} = -p\mathbf{1} + \mu\mathbf{A}_1 + \alpha_1\mathbf{A}_2 + \alpha_2\mathbf{A}_1^2 + \beta_3(\mathrm{tr}\,\mathbf{A}_1^2)\mathbf{A}_1. \tag{6}$$

If the normal stress parameters α_1 and α_2 are zero, then

$$\mathbf{T} = -p\mathbf{1} + (\mu + \beta_3\,\mathrm{tr}\,\mathbf{A}_1^2)\mathbf{A}_1, \tag{7}$$

where the quantity in the parenthesis can be thought of as an effective shear-dependent viscosity. Mansutti and Rajagopal [9] and Mansutti et al. [49] generalized Eq. (7) to obtain a power-law-type model:

$$\mathbf{T} = -p\mathbf{1} + \mu_0(\mathrm{tr}\,\mathbf{A}_1^2)^m\mathbf{A}_1, \tag{8}$$

where m is the power-law exponent; when $m < 0$, the fluid is shear thinning, while if $m > 0$ the fluid is shear thickening. Therefore, we can see that one of the shortcomings of the grade-type fluids, i.e., their inability to have shear dependent viscosity can be overcome by a generalization of a type given by Eq. (8). Similarly, if we go to Eq. (1) and assume $\beta_1 = \beta_2 = \beta_3 = 0$, we obtain the model for the second grade fluid

$$\mathbf{T} = -p\mathbf{1} + \mu\mathbf{A}_1 + \alpha_1\mathbf{A}_2 + \alpha_2\mathbf{A}_1^2. \tag{9}$$

This model also has a constant shear viscosity. Man and Sun [10] presented a modified form of Eq. (9) so that the viscosity could depend on the rate of deformation:

$$\mathbf{T} = -p\mathbf{1} + \mu[\tfrac{1}{2}\mathrm{tr}\,\mathbf{A}_1^2]^{m/2}\mathbf{A}_1 + \alpha_1\mathbf{A}_2 + \alpha_2\mathbf{A}_1, \tag{10}$$

when m is a material parameter, similar to Eq. (8). Gupta and Massoudi [11] generalized this relationship even further by assuming a temperature-dependent viscosity of the type

$$\mu(\theta) = \mu_0\mathrm{e}^{-M\theta}. \tag{11}$$

From this brief discussion, we can see that by giving an appropriate structure to the viscosity of a second-grade fluid (cf. Eq. (10)), we not only can have the normal stress effects but also a shear-dependent viscosity. Therefore, in Eq. (10), if $\alpha_1 = \alpha_2 = 0$, we have

$$\mathbf{T} = -p\mathbf{1} + \mu\{\tfrac{1}{2}\mathrm{tr}\,\mathbf{A}_1^2\}^{m/2}\mathbf{A}_1. \tag{12}$$

Now, a power-law fluid (cf. [12, p. 44]) in its properly frame-invariant form is given by

$$\mathbf{T} = -p\mathbf{1} + \eta(\gamma)\mathbf{A}_1, \tag{13}$$

where $\gamma = \sqrt{2\,\mathrm{tr}\,\mathbf{D}^2}$, $\mathbf{D} = \frac{1}{2}\mathbf{A}_1$, and

$$\eta(\gamma) = K(\gamma)^{n-1}, \tag{14}$$

where K and η are parameters that need to be determined empirically. A comparison of these equations reveal that $m = n - 1$ and $K = \mu$.

In the last few decades, interest in the boundary layer flow of non-Newtonian fluids, whether the second-grade fluids, or the power-law fluids has increased (cf. Srivatsava [13], Rajeswari and Rathna [14], Beard and Walters [15] for the early works on the grade-type fluids and Acrivos et al. [16] and Schowalter [17] for the early works on the power-law fluids). The boundary layer problems that have been studied, using a grade-type fluid, are the stagnation flow, flow over a flat plate, and flow over a stretching sheet. Rajagopal et al. [18] gave one of the first systematic approaches to the boundary layer flow of second-grade fluids. Rajagopal et al. [19] gave non-similar solutions for flow of a second-grade fluid over a wedge. Rajagopal et al. [20] studied the flow of such a fluid over a stretching sheet. Rajagopal and Gupta [20] obtained an exact solution for the same fluid over a porous plate. These works were followed by Rajagopal et al. [21] where non-similar solutions were obtained for flow over a stretching sheet with uniform flow stream. These studies motivated Massoudi and Ramezan [22,23] to look at the effect of injection or suction on the flow and heat transfer of second-grade fluids. Garg and Rajagopal [24] also provided a pseudo-similarity solution for flow of a second-grade fluid over a wedge. In recent years, Pakdemirli [25,26] has provided extensive studies for the boundary layer flows of non-Newtonial fluids. At the same time, Hsu et al. [27–29] have looked at the flow and heat transfer problems involving a second-grade fluid over a wedge and triangular fins. (cf. [50] [51] and [52] for additional studies).

For the power-law fluids, due to their simplicity, there has been more similar and non-similar solutions for boundary layers over external surfaces starting with the works of Schowalter [17] and Acrivos et al. [16]. A very thorough and updated review of this subject is given by Pakdemirli [25]. The effect of wall mass injection on the flow of a non-Newtonian fluid over a flat plate was investigated by Thompson and Snyder [30]. The interesting result from this problem was that of drag reduction at the wall due to injection. It was observed that a similarity solution existed only if the injection velocity had an x variation of the form $v_w \sim x^{-n/(1+n)}$.

Numerical results were presented for the velocity profiles, skin-friction coefficient, displacement thickness parameter, and momentum thickness parameter for n values in the range $0.1 \leqslant n \leqslant 2.5$ and mass injection parameter in the range 10^{-4}–1.0. The primary reason for studying the effect of injection is that this is one of the mechanisms to reduce the drag at the surface (cf. [31–35]).

Later Kim and Eraslan [36] studied the boundary-layer flow of a power-law fluid over wedges with wall mass injection consistent with the condition for the existence of similarity solutions. It was indicated that this condition corresponded to the injection velocity variation of the form $v_w \sim x^{(m(2n-1)-n)/(n+1)}$. Numerical results were presented for the velocity profiles and skin friction coefficient for two different wedge angle parameters, $\frac{1}{3}$ and $\frac{1}{6}$, for $0.25 \leqslant n \leqslant 1.5$. It was concluded that drag could be reduced considerably by the wall mass injection, and the degree of the reduction depended on the non-Newtonian flow index, but not directly on the wedge angle.

One of the few similarity solutions for the non-Newtonian fluid thermal boundary layers was reported by Lee and Ames [37]. The major difficulty encountered in analyzing non-Newtonian fluid systems stems from the non-linearities in the equation of motion. This factor limits the applicability of similarity analysis to the energy equation. It was concluded that the energy equation for external flow of power-law fluids with forced convection admits similarity solutions only for very restricted conditions: the flows about an isothermal, right angle wedge ($m = \frac{1}{3}$) and the flow past a flat plate ($m = 0.0$). Later, Thompson and Snyder [38] considered the problem of laminar velocity and thermal boundary layers in power-law fluids past external surfaces with surface fluid injection or suction. They presented data for the case of a flat plate with uniform wall temperature. Their approach was that of obtaining solutions of the momentum equation which were completely similar and of the energy equation which were similar in the sense of local similarity.

One frequently used concept in the solution of non-similarity boundary layer is the principle of local similarity. In this approach, the boundary layer equations are transformed, using suitable transformation, and divested of non-similar terms, are then applied locally and independently at different streamwise locations. Sparrow et al. [39] studied the causes of non-similarities. Three different cases were considered: non-similarity caused by (a) spatial variations in the freestream velocity, (b) surface mass transfer, and (c) transverse curvature. They introduced the method of local non-similarity and indicated that this method preserved the most attractive aspects of the local similarity model; that is, local solutions which are independent of the upstream information are obtainable and the partial differential equations are reduced to ordinary differential equations. Several boundary-layer velocity problems were solved, including Howarth's retarded flow, cylinder in crossflow, flat plate with uniform surface mass transfer, and cylinder in longitudinal flow. The three-equation model and two-equation model of the local non-similarity method showed excellent agreement with that of the finite difference method by Catherall et al. [40] when the skin friction was plotted versus the dimensionless streamwise coordinate ξ for the flow over of a flat plate with uniform blowing at the surface placed in an incompressible Newtonian fluid.

Afterwards, Sparrow and Yu [41] investigated a class of thermal boundary-layer problems which do not admit similarity solutions. Specifically, they dealt with the solution of non-similar boundary layers in the presence of surface mass transfer, transverse curvature, streamwise variation of the freestream velocity, and streamwise variation of the surface temperature. One classic example, which is related to our study, was that of a flat plate aligned parallel to a uniform freestream flow, with x denoting the streamwise coordinate and y the transverse coordinate. It is known that if there is surface mass transfer characterized by an injection velocity $v_w \sim x^{-1/2}$, then the similarity solutions are possible. Otherwise the velocity boundary layer would be non-similar. In particular, the case of uniform mass transfer was studied and temperature profiles and local heat transfer coefficients were presented. The three- and two-equation model of the local non-similarity thermal boundary-layer equations are in excellent agreement with a series solution which was performed by Wanous et al. [42] when the local heat transfer coefficients were plotted versus the dimensionless streamwise coordinate ξ for the flat plate with uniform surface mass transfer.

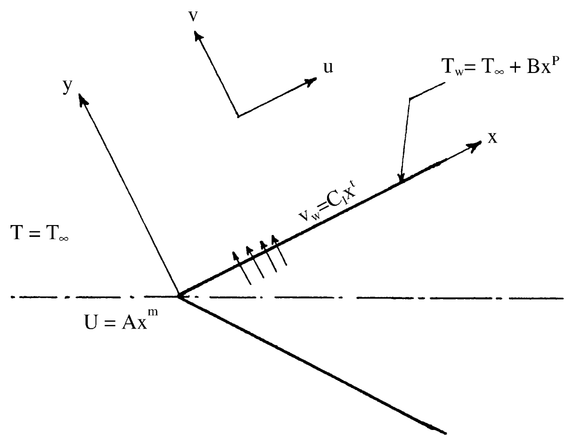

Fig. 1. System coordinates and geometry.

2. Statement of problem

The problem that we will study is the steady-state, laminar forced convection heat transfer for a non-isothermal wedge with arbitrary lateral mass transfer placed in a power-law non-Newtonian incompressible fluid. Fig. 1 illustrates the geometry of the problem and the corresponding coordinate system. The surface mass injection velocity and the wall temperature variations are considered to be of the arbitrary power-law forms. Results for the skin friction, temperature distribution, and local heat transfer coefficients are to be determined for two different Prandtl numbers. The effect of non-Newtonial flow index, variations of wall temperature and wall mass injection for a flat plate and a right angle wedge on the thermal characteristics of the flow are also examined.

Among the methods available for solving thermal boundary-layer problems which do not admit similarity solutions, the method of local similarity seems to be the one most frequently used, owing to its conceptual and computational simplicity. One interesting aspect of the local similarity method is that the solution at a particular streamwise location can be found without having to perform calculations at upstream locations. A second advantage of this method is that once the governing equations are transformed properly, they could be treated as ordinary differential equations and resemble those for similarity boundary layers. However, as Sparrow and Yu [41] have mentioned, one serious problem in applying the local-similarity method is that the results it provides are of uncertain accuracy. The main reason is thought to be the discarding of certain streamwise derivatives in the transformed governing equations, and there seems to be no clear way to establish the effect of these simplifications on the final results. The devised local non-similarity method not only preserves the two attractive features of the local similarity method outlined above, but also retains all terms in the momentum and energy equations. In contrast to the local-similarity method where certain terms were deleted in the momentum and energy equation, this approach deletes certain prescribed terms only from the subsidiary equations (auxiliary equations). Based on this, it is expected that the local non-similarity approach should give more accurate results than those from local similarity solutions. This issue and other relevant matters are discussed in the books by Na [43], and Seshadri and Na [44].

3. Governing equations

The basic governing equations are the conservation of mass, the conservation of linear momentum, and the energy equation. These are

$$\frac{\partial \rho}{\partial t} + \operatorname{div}(\rho \mathbf{v}) = 0, \tag{15}$$

$$\rho \frac{\mathrm{d}\mathbf{v}}{\mathrm{d}t} = \operatorname{div}\mathbf{T} + \rho \mathbf{b}, \tag{16}$$

$$\rho \frac{\mathrm{d}\varepsilon}{\mathrm{d}t} = \mathbf{T}\cdot\mathbf{L} - \operatorname{div}\mathbf{q} + \rho r, \tag{17}$$

where ρ is the density, $\mathbf{b}$ is the body force, ε is the specific internal energy, $\mathbf{L}$ is the velocity gradient, $\mathbf{q}$ is the heat flux vector, and r is the radiant heating. Since we are assuming that the fluid can undergo only isochoric motion, Eq. (15) reduces to

$$\operatorname{div}\mathbf{v} = 0. \tag{18}$$

The term $\mathbf{T}\cdot\mathbf{L}$ represents the viscous dissipation. We neglect the effect of radiation and assume that $\mathbf{q}$ is given by the Fourier's conduction law

$$\mathbf{q} = -k \operatorname{grad} T, \tag{19}$$

where T is the temperature, and k is the thermal conductivity, which is assumed to be constant, and the stress tensor $\mathbf{T}$ is given by Eq. (13). Substituting Eqs. (13) and (19) in (16) and (17), and making the appropriate assumptions within the boundary layer theory (cf. [45]), in Cartesian coordinates, the conservation of mass, the boundary layer, and the energy equations become, respectively,

$$\frac{\partial u}{\partial x} + \frac{\partial v}{\partial y} = 0, \tag{20}$$

$$u\frac{\partial u}{\partial x} + v\frac{\partial u}{\partial y} = U\frac{\mathrm{d}u}{\mathrm{d}x} + \frac{1}{\rho}\frac{\partial \tau_{xy}}{\partial y}, \tag{21}$$

$$u\frac{\partial T}{\partial x} + v\frac{\partial T}{\partial y} = \alpha\frac{\partial^2 T}{\partial y^2}, \tag{22}$$

where u and v are the velocity components along the direction of the flow and normal to the flow, respectively, T is the temperature and α is the thermal diffusivity.

The boundary conditions are given as

at $y = 0$ (at the wall):

$$u = 0, \quad v = v_{\mathrm{w}}(x), \quad T = T_{\mathrm{w}}(x) \tag{23}$$

and as $y \to \infty : u = U(x), \quad T = T_{\infty}.$ (24)

The first term on the right-hand side of the momentum equation (21) represents the effect of the axial pressure gradient which exists due to the variable velocity $U(x)$ of the external flowstream.

3.1. Transformation of the governing equations

The first step in the development of this method is to transform the governing equations from the x, y coordinate system to ξ, η system. The coordinate η, which involves both x and y would be a similarity variable if the boundary-layer were similar. However, ξ is related to x alone and is so chosen that x does not appear explicitly in the transformed equations. As Sparrow and Yu [41] indicate: "the transformation tends to remove the streamwise dependence associated with the natural growth of the boundary layer, such as occurs for similarity boundary layer. Therefore, the remaining streamwise dependence is due to the non-similarity." Hence, in general, x and y could be transformed to ξ and η by

$$x \to \xi = Hx^a, \quad y \to \eta = Gyx^r, \tag{25}$$

where H, a, C, and r are constants to be determined. Let us introduce the generalized stream function ψ as

$$\psi = Dx^s f(\xi, \eta) \tag{26}$$

and dimensionless temperature θ as

$$\theta(\xi, \eta) = \frac{T - T_\infty}{T_w - T_\infty}, \tag{27}$$

where D and s are to be determined. Noting that

$$u = \frac{\partial \psi}{\partial y} \quad \text{and} \quad v = \frac{-\partial \psi}{\partial x}, \tag{28}$$

the conservation of mass, Eq. (20) is identically satisfied.

The mainstream velocity, the surface mass injection velocity and wall temperature variations are considered to be of the arbitrary power-law forms. Therefore,

$$U(x) = Ax^m, \tag{29}$$

$$v_w(x) = C_1 x^t, \tag{30}$$

$$T_w(x) = T_\infty + Bx^p, \tag{31}$$

where A, C_1, B, m, t, p, and T_∞ are constants.

Substituting Eqs. (25)–(31), using (13) and (14) into (20)–(24) yields

$$(f'')^{n-1}f''' + \phi ff'' + \beta[1 - (f')^2] = \frac{a\phi\xi}{s}\left(f'\frac{\partial f'}{\partial \xi} - f''\frac{\partial f}{\partial \xi}\right) \tag{32}$$

and

$$\left(\frac{1}{\Pr}\right)\theta'' + 2\xi^{(s-r-1)/a}(sf\theta' - pf'\theta) = 2a\xi^{((s-r-1)/a)+1}\left(f\frac{\partial \theta}{\partial \xi} - \theta'\frac{\partial f}{\partial \xi}\right) \tag{33}$$

with the boundary conditions

$$\text{at } \eta = 0, \tag{34a}$$

$$f'(\xi, 0) = 0, \tag{34b}$$

$$f(\xi, 0) + \xi = \frac{-a}{s}\xi\frac{\partial f(\xi, 0)}{\partial \xi}, \tag{34c}$$

$$\theta(\xi, 0) = 1, \tag{34d}$$

$$\text{at } \eta \to \infty, \quad f'(\xi, \infty) = 1, \quad \theta(\xi, \infty) = 0, \tag{35}$$

where

$$r = \frac{m(2-n) - 1}{n+1}, \quad s = \frac{m(2n-1) + 1}{n+1},$$

$$a = t - s + 1,$$

$$C = \left\{\frac{\rho}{2K}A^{2-n}[1 + m(2n-1)]\right\}^{1/(n+1)},$$

$$D = A/C, \quad H = \frac{C_1 C}{sA}, \quad \Pr = \frac{D}{2\alpha C}H^{(1-s+r)/a}$$

$$\phi = \frac{2}{n(n+1)}, \quad \beta = \frac{2m}{n[1 + m(2n-1)]}. \tag{36}$$

3.2. Similarity solutions for special cases

For the sake of completeness and comparison with local similarity and local non-similarity methods, in this section we attempt to find the conditions at which similar solutions may exist for certain special cases. With the following transformations, noting that η is now the similarity variable,

$$\eta = Cyx^r, \quad \psi = Dx^s f(\eta), \quad \theta(\eta) = \frac{T - T_\infty}{T_w - T_\infty} \tag{37}$$

with

$$T_w - T_\infty = Bx^p, \quad U(x) = Ax^m, \quad v_w = C_1 x^t, \tag{38}$$

the governing equations (21) and (22) and the boundary conditions reduce to

$$(f'')^{n-1}f''' + \frac{s}{(Kn/\rho)C^{2n-1}D^{n-2}}x^{r-2nr+2s-ns-1}ff'' - \frac{r+s}{(Kn/\rho)C^{2n-1}D^{n-2}}x^{r-2nr+2s-ns-1}(f')^2 + \frac{A^2m}{(Kn/\rho)C^{2n+1}D^n}x^{2m-1-2nr-ns} = 0, \tag{39}$$

$$\theta'' + \frac{Ds}{\alpha C}x^{s-r-1}f\theta' - \frac{Dp}{\alpha C}x^{s-r-1}\theta f' = 0 \tag{40}$$

with

$$f'(0) = 1, \tag{41a}$$

$$f(0) = -\left(\frac{C_1}{Ds}\right)x^{t-s+1}, \tag{41b}$$

$$f'(\infty) = 1, \tag{41c}$$

$$\theta(0) = 1, \quad \theta(\infty) = 0. \tag{42}$$

To have similarity solutions, it is required that the exponents of x in (39)–(41b) must vanish, that is,

$$r - 2nr + 2s - ns - 1 = 0, \tag{43a}$$

$$2m - 1 - 2nr - ns = 0, \tag{43b}$$

$$s - r - 1 = 0, \tag{43c}$$

$$t - s + 1 = 0. \tag{43d}$$

Solving for r and s from (43a) and (43b) gives

$$r = \frac{m(2-n)-1}{n+1}, \quad s = \frac{1-m(1-2n)}{n+1}. \tag{44}$$

It follows immediately by substituting (44) into (43c) and (43a) that similarity solutions exist only for the following two special cases:

(i) when the fluid is Newtonian ($n = 1.0$):

$$t = \frac{m-1}{2} \quad \text{for } n = 1.0, \tag{45}$$

(ii) when the fluid is non-Newtonian:

$$t = -\frac{1}{3}, \quad m = \frac{1}{3} \quad \text{for arbitrary } n. \tag{46}$$

These restrictions agree with the case of Newtonian flow past a flat plate ($n = 1$ and $m = 0$) reported by Hartnett and Eckert [46] and the case of non-Newtonian flow over a right-angle wedge ($m = \frac{1}{3}$) studied by Lee and Ames [37].

3.3. Local similarity solutions

As was just indicated, the energy equation with injection at the surface admits similarity solution for a few restricted cases. Before proceeding with the local non-similarity solution method, it is useful to review the method of local similarity. According to this approach, the right-hand sides of Eqs. (32)–(34b) are assumed to be small enough so that they could be approximated by zero. Hence, the boundary-layer equations and the boundary conditions become

$$(f'')^{n-1}f''' + \phi ff'' + \beta[1 - f'^2] = 0, \tag{47}$$

$$\left(\frac{1}{\mathrm{Pr}}\right)\theta'' + 2\xi^{(s-r-1)/a}(sf\theta' - Pf'\theta) = 0 \tag{48}$$

with

$$f(\xi,0) = -\xi, \quad f'(\xi,0) = 0, \quad f'(\xi,\infty) = 1 \tag{49}$$

and

$$\theta(\xi,0) = 1, \quad \theta(\xi,\infty) = 0. \tag{50}$$

The quantity ξ may be regarded as a constant parameter at any streamwise location. Thus Eqs. (47) and (48) can be treated as ordinary differential equations and solved at different locations ξ using a modified version of the scheme developed by Nachtsheim and Swigert [47]. It should be noted that the solution corresponding to a given particular ξ is independent of the solution at any other ξ. As a result, the accuracy of the results is uncertain as ξ increases. In fact, it is quite poor at large injection rates (large ξ) [39,41].

3.4. Local non-similarity solutions

Using the method of local non-similarity (cf. [39]), let

$$g(\xi,\eta) = \frac{\partial f(\xi,\eta)}{\partial \xi} \tag{51}$$

and

$$h(\xi,\eta) = \frac{\partial\theta(\xi,\eta)}{\partial\xi}. \tag{52}$$

Substituting these quantities into the governing equations and boundary conditions, (32)–(36), gives

$$(f'')^{n-1}f''' + \phi ff'' + \beta[1 - f'^2] = \frac{a\phi}{s}\xi(f'g' - f''g) \tag{53}$$

with

$$f + \xi = \frac{-a}{s}\xi g \quad f'(\xi,0) = 0,$$

$$f'(\xi,\infty) = 1, \quad \text{at } \eta = 0, \tag{54}$$

and

$$\left(\frac{1}{\mathrm{Pr}}\right)\theta'' + 2\xi^{(s-r-1)/a}(sf\theta' - pf'\theta)$$
$$= 2a\xi^{(s-r+a-1)/a}(f'h - \theta'g) \tag{55}$$

with

$$\theta(\xi,0) = 1, \quad \theta(\xi,\infty) = 0, \tag{56}$$

where again primes denote differentiation with respect to η. Next, Eqs. (53)–(56) are differentiated with respect to ξ, yielding

$$(f'')^{n-1}g''' + [(n-1)(f'')^{n-2}f''' + \phi f]g''$$
$$-\left(2\beta + \frac{a\phi}{s}\right)f'g' + \left(\phi + \frac{a\phi}{s}\right)f''g$$
$$= \frac{a\phi}{s}\xi\frac{\partial}{\partial\xi}(f'g' - f''g) \tag{57}$$

with

$$\left(1 + \frac{a}{s}\right)g + 1 = \frac{-a}{s}\xi\frac{\partial g}{\partial\xi}, \tag{58a}$$

$$g'(\xi,0) = 0, \tag{58b}$$

$$g'(\xi,\infty) = 0 \tag{58c}$$

and

$$\left(\frac{1}{\mathrm{Pr}}\right)h'' + 2\xi^{(s-r-1)/a}sfh' - 2(p+s+a-r-1)$$
$$\times\,\xi^{(s-r-1)/a}f'h + 2\xi^{(s-r-1)/a}\left[\left(\frac{s-r-1}{a}\right)\frac{s}{\xi}f\right.$$
$$\left. + (2s-r+a-1)g\right]\theta'$$
$$-\,2p\xi^{(s-r-1)/a}\left[\left(\frac{s-r-1}{a}\right)\frac{1}{\xi}f' + g'\right]\theta$$
$$= 2a\xi^{(s-r+a-1)/a}\frac{\partial}{\partial\xi}[f'h - \theta'g] \tag{59}$$

with

$$h(\xi,0) = 0, \quad h(\xi,\infty) = 0. \tag{60}$$

Eqs. (57)–(60) serve as auxiliaries to the governing equations with their boundary equations (53)–(56). As discussed by Sparrow and Yu [41], it is assumed that the right-hand side of the auxiliary equations (57), (58b), and (59), are sufficiently small so that they may be neglected. With the above assumption, the momentum boundary-layer equation (53) and its auxiliary equation (57) could be brought together with their boundary conditions as

$$(f'')^{n-1}f''' + \phi ff'' + \beta(1 - f'^2) = \frac{a\phi}{s}\xi(f'g' - f''g), \tag{61}$$

$$(f'')^{n-1}g''' + [(n-1)(f'')^{n-2}f''' + \phi f]g''$$
$$-\left(2\beta + \frac{a\phi}{s}\right)f'g' + \left(\phi + \frac{a\phi}{s}\right)f''g = 0 \tag{62}$$

with

$$f(\xi,0) = -\frac{s}{a+s}\xi, \quad g(\xi,0) = -\frac{s}{a+s},$$

$$f'(\xi,0) = 0, \quad g'(\xi,0) = 0, \tag{63}$$

$$f'(\xi,\infty) = 1, \quad g'(\xi,\infty) = 0. \tag{64}$$

When ξ is regarded as a constant parameter, Eqs. (61)–(64) may be treated as a system of ordinary differential equations to be solved numerically.

In a similar manner, the thermal boundary-layer equation (55) and its auxiliary equation (59) could be brought together with their boundary conditions as

$$\left(\frac{1}{\mathrm{Pr}}\right)\theta'' + 2\xi^{(s-r-1)/a}(sf\theta' - pf'\theta) = 2a^{(s-r+a-1)/a}(f'h - \theta' g), \quad (65)$$

$$\left(\frac{1}{\mathrm{Pr}}\right)h'' + 2\xi^{(s-r-1)/a}sfh' - 2(p+s+a-r-1) \times \xi^{(s-r-1)/a}f'h + 2\xi^{(s-r-1)/a}\left[\left(\frac{s-r-1}{a}\right)\frac{s}{\xi}f + (2s-r+a-1)g\right]\theta' - 2p\xi^{(s-r-1)/a}\left[\left(\frac{s-r-1}{a}\right)\frac{1}{\xi}f' + g'\right]\theta = 0 \quad (66)$$

with

$$\theta(\xi,0) = 1, \quad h(\xi,0) = 0, \quad (67)$$

$$\theta(\xi,\infty) = 0, \quad h(\xi,\infty) = 0. \quad (68)$$

Again for a fixed value of ξ, Eqs. (67)–(68) may be treated as a set of ordinary differential equations, with the velocity functions f, f', g, and g' as input. A description of the numerical scheme developed to solve the above equations is given in Massoudi [48].

4. Results and discussion

4.1. Velocity profiles and skin-friction coefficient

The governing equations for the fluid velocity distribution, Eqs. (61) and (62) with boundary conditions (63)–(64) are solved using a modified version of the scheme developed by Nachtsheim and Swigert [47]. Numerical results are obtained for three flow indices, $n = 0.5$, 1.0, 1.2, two injection indices $t = 0$, 1.0, and two wedge angles, $m = 0, \frac{1}{3}$.

The dimensionless velocity profiles are shown in Figs. 2a–c for a constant fluid injection ($t = 0$) and in Figs. 3a–c for a linear injection ($t = 1.0$). As expected in both cases, the velocity boundary layers over a right-angle wedge ($m = \frac{1}{3}$) are thinner than those along a flat plate ($m = 0$). The effect of the fluid injection is also clearly shown. At fixed values of m, n, and t, the wall slope of these curves, and hence the wall friction, decreases with increasing injection. This trend is more pronounced for the pseudoplastic fluid ($n = 0.5$) than for the dilatant fluid ($n = 1.2$).

Fig. 4 shows the effects of t and ξ on the dimensionless velocity profiles for the case of a Newtonian fluid ($n = 1.0$) past a flat plate ($m = 0.0$). It is noted that the injection index t represents the variation of injection along the wall, whereas the injection parameter ξ represents the dimensionless injection rate with a prescribed wall injection variation. It is seen from Fig. 4 that t and ξ have a significant destabilizing effect on the velocity distribution. The successive profiles become increasingly S-shaped with increasing ξ or decreasing t. Physically, this trend is due to the gradual lift-off of the boundary-layers at higher injection rates or with the variation changes from linear injection ($t = 1.0$) to negative-exponent injections ($t = -\frac{1}{3}$ and $-\frac{1}{2}$).

The local skin-friction coefficient C_{fx} is calculated from the following equation:

$$C_{\mathrm{fx}} = \frac{(\tau_{xy})_{y=0}}{(1/2)\rho u^2} = \left(\frac{2}{\mathrm{R_{ex}}}\right)^{1/(n+1)}[1 + m(2n-1)]^{n/(n+1)}[f''(\xi,0)]^n, \quad (69)$$

where $\mathrm{R_{ex}} = (\rho/K)U^{2-n}x^n$ is the Reynolds number. The results are shown in Fig. 5. The coefficient decreases as the injection rate increases and C_{fx} increases for the accelerated-flow case ($m = \frac{1}{3}$) as compared to the flat plate case ($m = 0$). These trends are in agreement with those for Newtonian boundary layer studies. For non-Newtonian fluids studied here, it is observed that the local skin-friction coefficient decreases with increasing n. As compared to the case of uniform injection ($t = 0$), the effect of a linear-injection ($t = 1.0$) becomes increasingly significant at higher wall injection rates.

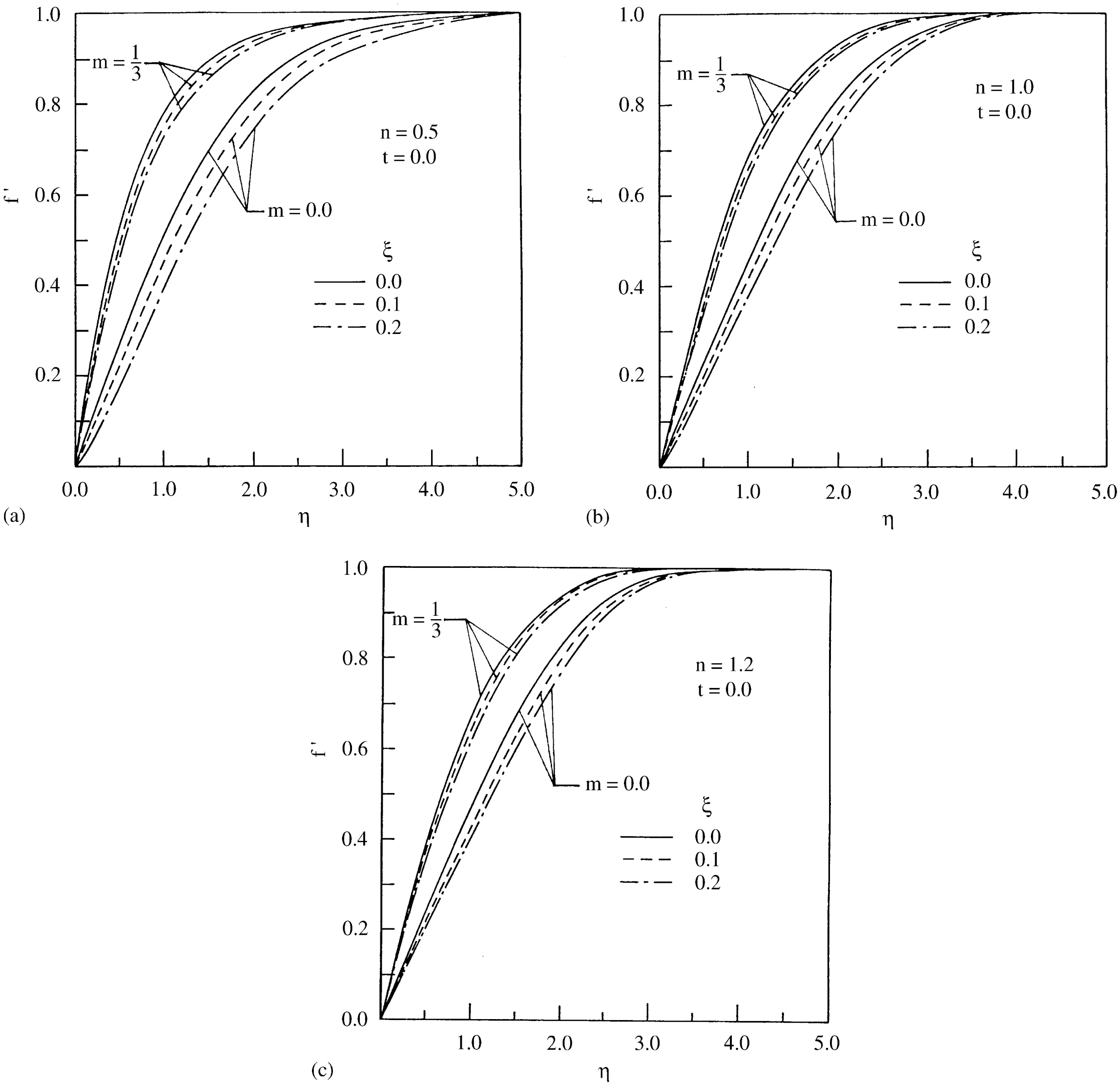

Fig. 2. (a) Dimensionless velocity profiles for $n = 1.0$ and $t = 0$. (b) Dimensionless velocity profiles for $n = 1.0$ and $t = 0$. (c) Dimensionless velocity profiles for $n = 1.2$ and $t = 0$.

4.2. Thermal characteristics

The governing equations for the fluid temperature distribution, Eqs. (65) and (66) with boundary conditions (67) and (68) are solved using a similar scheme to the one just mentioned for the momentum boundary-layer equations. Numerical results are obtained for fluids with Prandtl numbers 0.7 and 10.0 for isothermal surfaces ($p = 0.0$) and surfaces with temperatures varying linearly with x ($p = 1.0$).

The dimensionless temperature profiles are presented in Figs. 6a–c for three cases of flow behavior indices at three different values of the dimensionless injection parameter ξ when $m = \frac{1}{3}$, $p = 1.0$, and $t = 1.0$. As anticipated, the thermal boundary layer

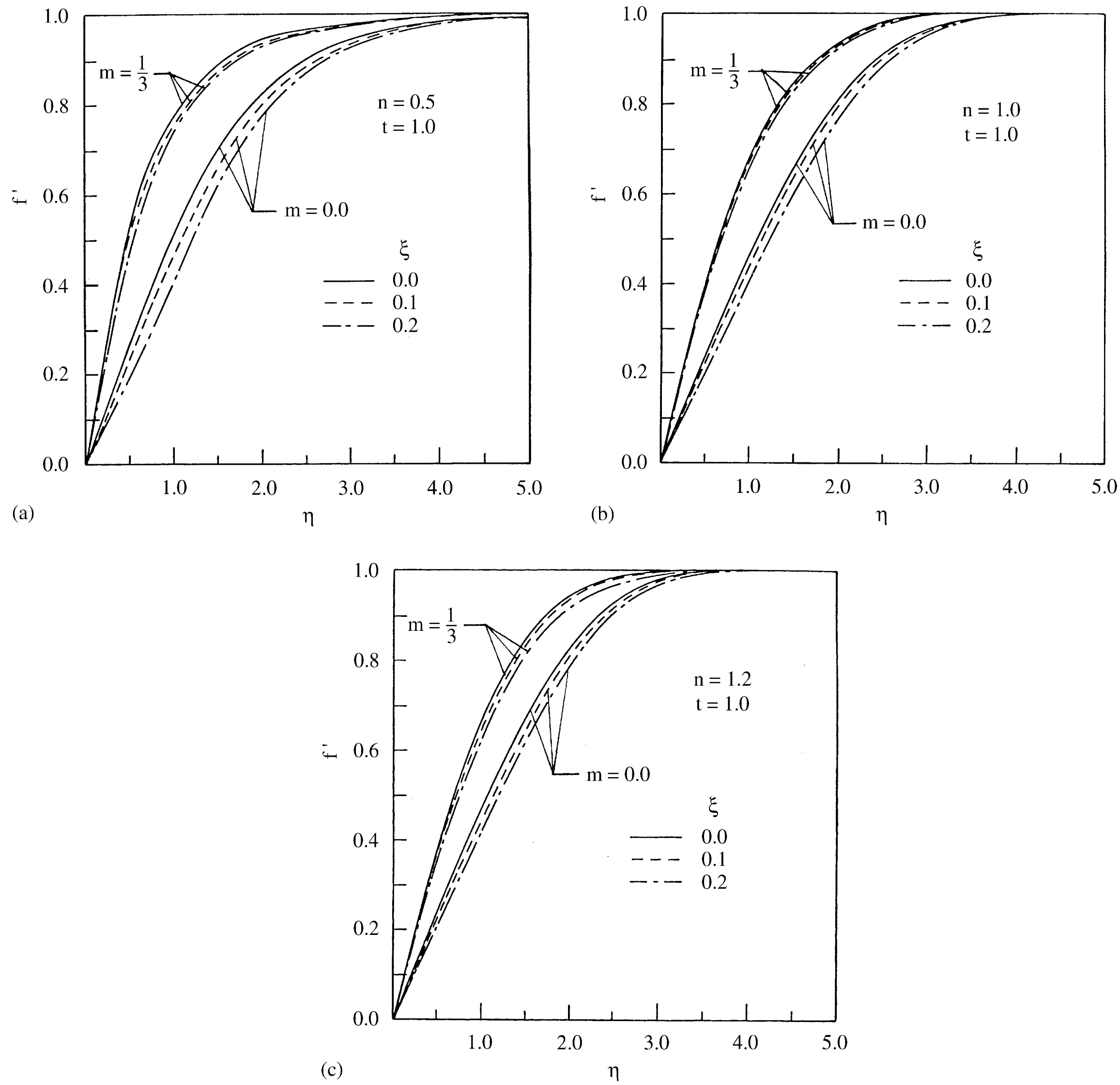

Fig. 3. (a) Dimensionless velocity profiles for $n = 0.5$ and $t = 1.0$. (b) Dimensionless velocity profiles for $n = 1.0$ and $t = 1.0$. (c) Dimensionless velocity profiles for $n = 1.2$ and $t = 1.0$.

thickness decreases with increasing Prandtl number. Fig. 7 compares the temperature profiles for three fluids, $n = 0.5, 1.0, 1.2$, over a flat plate ($m = 0$) and a right angle wedge ($m = \frac{1}{3}$). The results are presented for uniform injection, linear variation of surface temperature and Prandtl number 0.7 at the injection rate $\xi = 0.1$. In the case of a flat plate, the thermal boundary-layer thickness decreases as the non-Newtonian power-law exponent n increases. However, for the case of a right angle wedge (accelerated flow), $m = \frac{1}{3}$, the reverse behavior is observed.

The effects of injection index t, surface temperature variation parameter p, and wedge angle

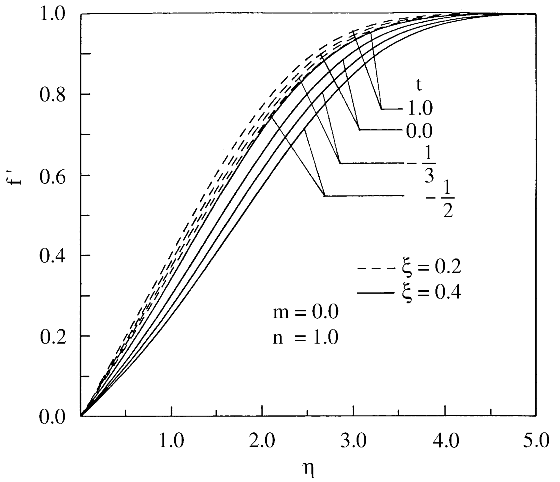

Fig. 4. Effect of non-uniform injection along a flat plate.

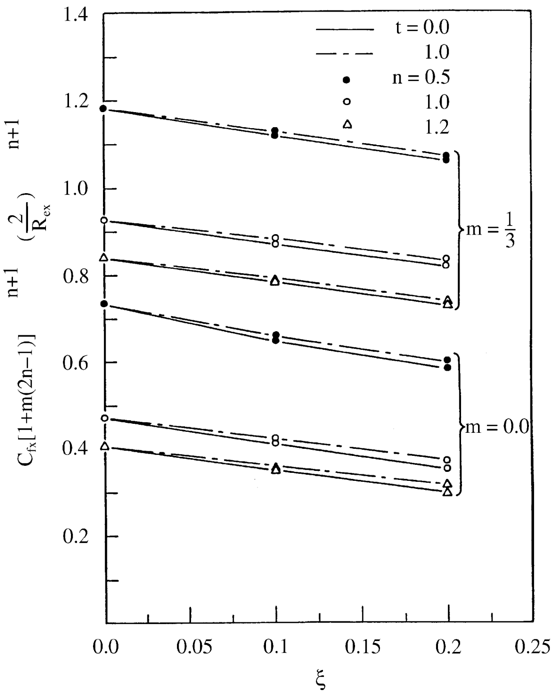

Fig. 5. Scaled local skin-friction coefficients.

parameter m may better be presented by introducing the local Nusselt number,

$$\mathrm{Nu}_x = \frac{h_1 x}{k}, \tag{70}$$

where h_1 is the local heat transfer coefficient defined by

$$h_1 = \frac{q}{T_x - T_\infty}. \tag{71}$$

From Fourier's Law

$$q = -k\left.\frac{\partial T}{\partial y}\right|_{y=0}. \tag{72}$$

Recalling that $T_w - T_\infty = Bx^p$, substituting Eqs. (71) and (72) in (70) we obtain

$$\mathrm{Nu}_x = -\left(\frac{\mathrm{Re}_x}{2}\right)^{1/(n+1)}[1 + m(2n-1)]^{1/(n+1)} \times \theta'(\xi, 0). \tag{73}$$

The variations of the Nu_x with ξ are presented in Fig. 8 for different values of m, p, t when $n = 1.0$ and $\mathrm{Pr} = 10$. The results clearly show the effect of injection index t. For a given value of m, for example $m = 0.0$, and for the isothermal case, $p = 0.0$, with uniform injection, $t = 0$, the Nu_x is reduced 68% when ξ is increased from 0.01 to 0.2. Similar behavior is observed for other values of m, p, and t, as shown in Fig. 8. For the case of linear surface temperature variation, $p = 1.0$, the local heat transfer coefficients are higher than those of the isothermal case, $p = 0.0$.

It is also noteworthy that for a given injection index t and a given surface temperature parameter p, the local Nusselt number is higher for the case of accelerated flow ($m = \frac{1}{3}$) over a right-angle wedge than for the case of a uniform flow over a flat plate ($m = 0$).

Fig. 9 shows the effects of n, m, ξ and Pr on the local Nusselt number. It increases with increasing n for $m = 0$ (flat plate), but decreases with increasing n for $m = \frac{1}{3}$ (right-angle wedge). For fixed values of n and m, it increases with increasing Pr as well as with decreasing injection rate ξ, the latter increase is much higher for $\mathrm{Pr} = 10$ than for 0.7.

It is noted that the energy equation, in general, does not possess solution at $\xi = 0.0$ except for the

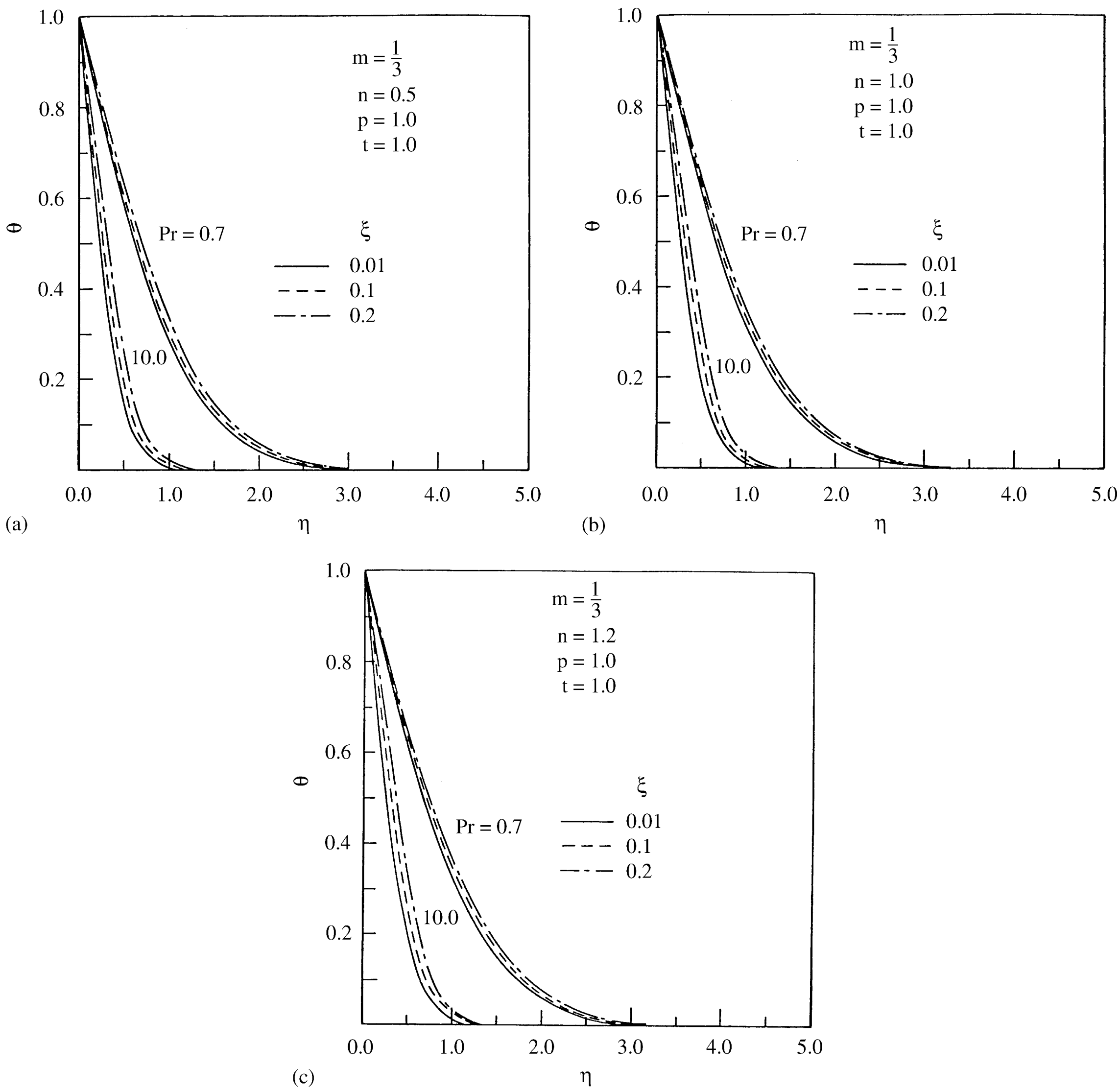

Fig. 6. (a) Dimensionless temperature profiles for $m = \frac{1}{3}$ and $n = 0.5$. (b) Dimensionless temperature profiles for $m = \frac{1}{3}$ and $n = 1.0$. (c) Dimensionless temperature profiles for $m = \frac{1}{3}$ and $n = 1.2$.

cases when $n = 1$ or $m = \frac{1}{3}$. In Figs. 6a–c, and 8 the results are presented at $\xi = 0.01$.

5. Conclusions

Heat transfer and laminar boundary layer flows of a non-Newtonian fluid over a porous wedge is studied. The free stream velocity, the injection velocity, and the surface temperature are assumed to be varying functions of the streamwise coordinate x. The non-Newtonian fluid model used is the power-law, properly put in the framework of fluids of differential type. Similarity, local similarity, and local non-similarity techniques are discussed, and various restrictions on velocity, temperature, and

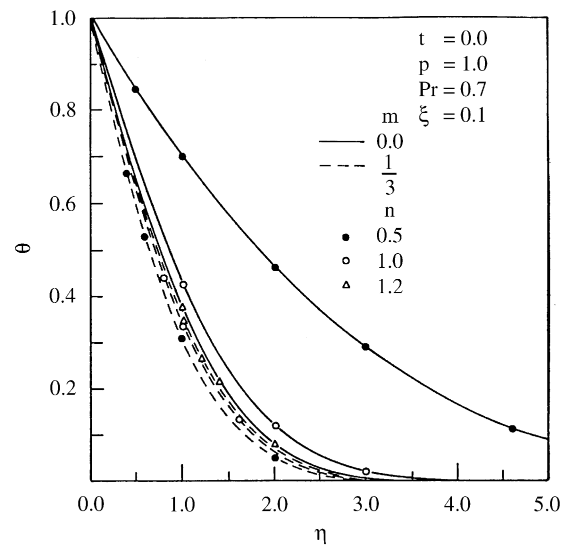

Fig. 7. Comparison of temperature profiles for different values of m and n.

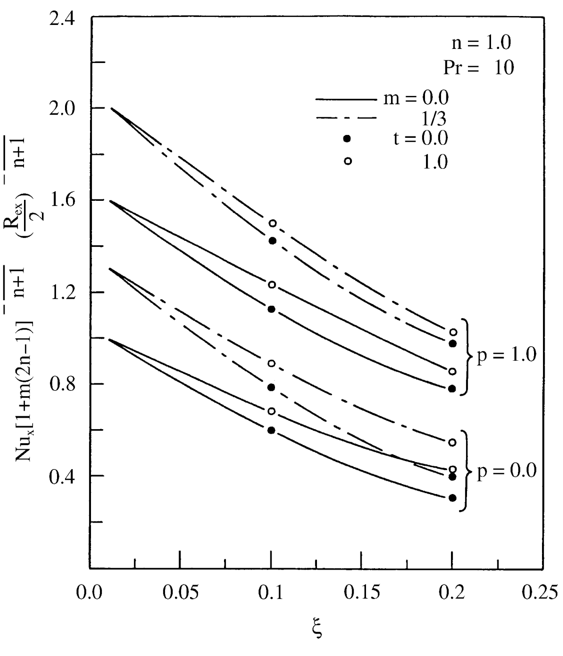

Fig. 8. Scaled local Nusselt number for $n = 1.0$ and $\mathrm{Pr} = 10.0$.

injection velocity parameters are also obtained. The effect of injection on drag reduction and the local heat transfer coefficient at the wall are also studied.

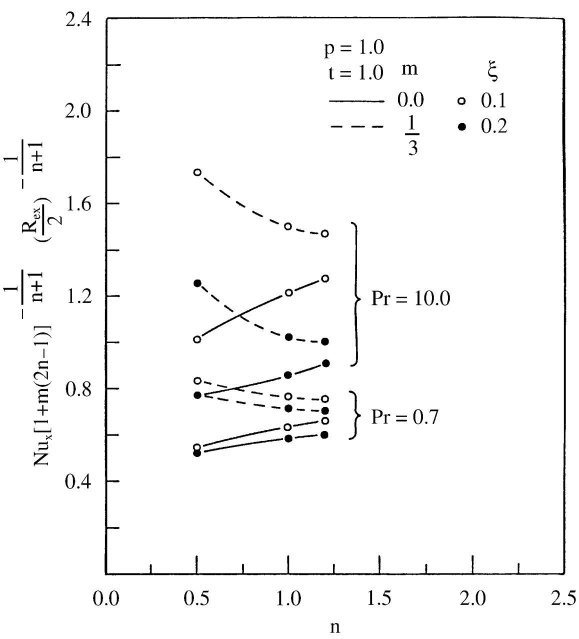

Fig. 9. Scaled local Nusselt number vs. n.

Acknowledgements

I am grateful to Professor K.R. Rajagopal for his many helpful comments. I would also like to thank Ms. Diana Maria of the Word Processing Center at NETL for typing the manuscript.

References

[1] R.S. Rivlin, J.L. Ericksen, Stress deformation relations for isotropic materials, J. Rational Mech. Anal. 4 (1955) 323.

[2] C. Truesdell, W. Noll, The Non-Linear Field Theories of Mechanics, 2nd edition, Springer, New York, 1992.

[3] J.G. Oldroyd, On the formulation of rheological equations of state, Proc. Roy. Soc. London A 200 (1950) 523.

[4] K.R. Rajagopal, A.R. Srinivasa, A thermodynamic frame work for rate type fluid models, J. Non-Newtonial Fluid Mech. 88 (2000) 207.

[5] J.E. Dunn, K.R. Rajagopal, Fluids of differential type: critical review and thermodynamic analysis, Int. J. Engng Sci. 33 (1995) 689.

[6] M. Reiner, Rheology, in Handbuch der Physik, Edited by S. Flügge, Vol. VI, Springer, Berlin, 1958.

[7] J.E. Dunn, R.L. Fosdick, Thermodynamics, stability and boundedness of fluids of complexity 2 and fluids of second grade, Arch. Rational Mech. Anal. 56 (1974) 191.

[8] R.L. Fosdick, K.R. Rajagopal, Thermodynamics and stability of fluids of third grade, Proc. Roy. Soc. London A 339 (1980) 351.
[9] D. Mansutti, K.R. Rajagopal, Flow of a shear thinning fluid between intersecting planes, Int. J. Non-Linear Mech. 26 (1991) 769.
[10] C.S. Man, Q.K. Sun, On the significance of normal stress effects in the flow of glaciers, J. Glaciol. 33 (1987) 268.
[11] G. Gupta, M. Massoudi, Flow of a generalized second grade fluid between heated plates, Acta Mech. 99 (1993) 21.
[12] J.C. Slattery, Advanced Transport Phenomena, Cambridge University Press, New York, 1999.
[13] A.C. Srivatsava, The flow of a non-Newtonian liquid near a stagnation point, ZAMP 9 (1958) 80.
[14] G. Rajeswari, S.L. Rathna, Flow of a particular class of non-Newtonian visco-elastic and visco-inelastic fluids near a stagnation point, ZAMP 13 (1962) 43.
[15] D.W. Beard, K. Walters, Elastico-viscous boundary layer flows, Proc. Cambridge Philos. Soc. 60 (1964) 667.
[16] A. Acrivos, M.J. Shah, E.E. Peterson, Momentum and heat transfer in laminar boundary-layer flow of non-Newtonian fluids past external surfaces, A.I.CH.E. J. 6 (2) (1960) 312–317.
[17] W.R. Schowalter, The application of boundary-layer theory to power-law pseudoplastic fluids: similarity solutions, A.I.CH.E. J. 6 (1960) 25.
[18] K.R. Rajagopal, A.S. Gupta, A.S. Wineman, On a boundary layer theory for non-Newtonian fluids, Lett. Appl. Engng Sci 18 (1980) 875.
[19] K.R. Rajagopal, A.S. Gupta, T.Y. Na, A note on the Falkner-Skan flows of a non-Newtonian fluid, Int. J. Non-Linear Mech. 18 (1983) 313.
[20] K.R. Rajagopal, A.S. Gupta, An exact solution for the flow of a non-Newtonian fluid past an infinite porous plate, Meccanica 19 (1984) 158.
[21] K.R. Rajagopal, T.Y. Na, A.S. Gupta, A non-similar boundary layer on a stretching sheet in a non-Newtonian fluid with uniform free stream, J. Math. Phys. Sci. 21 (1987) 189.
[22] M. Massoudi, M. Ramezan, Effect of injection or suction on the Falkner-Skan flows of second grade fluids, Int. J. Non-Linear Mech. 24 (1989) 221.
[23] M. Massoudi, M. Ramezan, Heat transfer analysis of a viscoelastic fluid at a stagnation point, Mech. Res. Commun. 19 (1992) 129.
[24] V.K. Garg, K.R. Rajagopal, Flow of a non-Newtonian fluid past a wedge, Acta Mech. 88 (1991) 113.
[25] M. Pakdemirli, Boundary layer flow of power-law fluids past arbitrary profiles, IMA J. Appl. Math. 50 (1993) 133.
[26] M. Pakdemirli, Conventional and multiple deck boundary layer approach to second and third grade fluids, Int. J. Engng Sci. 32 (1994) 141.
[27] C.H. Hsu, C.S. Chen, J.T. Teng, Temperature and flow fields for the flow of a second grade fluid past a wedge, Int. J. Non-Linear Mech. 32 (1997) 933.
[28] C.H. Hsu, K.L. Hsiao, J.T. Teng, Conjugate heat transfer of a triangular fin in the flow of a second-grade fluid, Int. J. Heat Fluid Flow 19 (1998) 282.
[29] C.H. Hsu, K.L. Hsiao, Conjugate heat transfer of a plate fin in a second-grade fluid flow, Int. J. Heat Mass Transfer 41 (1998) 1087.
[30] E.R. Thompson, W.T. Snyder, Drag reduction of a non-Newtonian fluid by fluid injection at the wall, Journal of Hydronautics 2 (4) (1968) 177–180.
[31] M. Akcay, M.A. Yukselen, Drag reduction of a non-Newtonian fluid by fluid injection on a moving wall, Arch. Appl. Mech. 69 (1999) 215.
[32] R. Latorre, Ship hull drag reduction using bottom air injection, Ocean Engng 24 (1997) 161.
[33] J.L. Lumley, Drag reduction by additives, Annu. Rev. Fluid Mech. 1 (1969) 367.
[34] M. Renardy, On the mechanism of drag reduction, J. Non-Newtonian Fluid Mech. 59 (1995) 93.
[35] K. Watanabe, Yanuar, H. Udagawa, Drag reduction of Newtonian fluid in a circular pipe with a highly water-repellent wall, J. Fluid Mech. 381 (1999) 225.
[36] H.H. Kim, A.H. Eraslan, Flow of a non-Newtonian fluid past wedges with wall mass injection, J. Hydronaut. 3 (1) (1969) 57–59.
[37] S.Y. Lee, W.F. Ames, Similarity solutions for non-Newtonian fluids, A.I.CH.E. J. 12 (4) (1966) 700–708.
[38] E.R. Thompson, W.T. Snyder, Laminar boundary-layer flows of power-law non-Newtonian fluids past external surfaces with mass and heat transfer, Proceedings of the 5th International Congress on Rheology, Kyoto, Japan, Vol. 1, October 1968, pp. 217–239.
[39] E.M. Sparrow, H. Quack, C.J. Boerner, Local non-similarity boundary-layer solutions, AIAA J. 8 (11) (1970) 1936–1942.
[40] D. Catherall, K. Stewartson, P.G. Williams, Viscous flow past a flat plate with uniform injection, Proceedings of Royal Society, Ser. A 284 (1398) (1965) 370–396.
[41] E.M. Sparrow, H.S. Yu, Local non-similarity thermal boundary-layer solutions, J. Heat Transfer Trans. ASME (1971) 328–334.
[42] K.J. Wanous, E.M. Sparrow, Heat transfer for flow longitudinal to a cylinder with surface mass transfer, J. Heat Transfer Trans. ASME Ser. C 87 (1) (1965) 317–319.
[43] T.Y. Na, Computational Methods in Engineering Boundary Value Problems, Academic Press, New York, 1979.
[44] R. Seshadri, T.Y. Na, Group Invariance in Engineering Boundary Value Problems, Springer, New York, 1985.
[45] H. Schlicting, Boundary Layer Theory, 7th Edition, McGraw-Hill, New York, 1979.
[46] J.P. Hartnett, E.R.G. Eckert, Mass-transfer cooling in a laminar boundary-layer with constant fluid properties, Trans. ASME 79 (1957) 247–254.
[47] P.R. Nachtsheim, P. Swigert, Satisfaction of asymptotic boundary conditions in numerical solutions of systems of non-linear equations of boundary-layer type, TN D-3004, NASA, 1965.
[48] M. Massoudi, Heat transfer in non-Newtonian fluids with mass injection. MS Thesis, University of Pittsburgh, 1981.

[49] D. Mansutti, G. Pontrelli, K.R. Rajagopal, Steady flow of non-Newtonian fluids past a porous plate with suction or injection, Int. J. Numer. Methods Fluids 17 (1993) 927.
[50] H.R. Nataraja, M.S. Sarma, B. Nagewara Rao, Non-similar solutions for flow and heat transfer in a viscoelastic fluid over a stretching sheet, Int. J. Non-Linear Mech. 33 (1998) 357.
[51] K.R. Rajagopal, A note on unsteady unidirectional flows of a non-Newtonian fluid, Int. J. Non-Linear Mech. 17 (1982) 369.
[52] K.R. Rajagopal, A.Z. Szeri, W. Troy, An existence theorem for the flow of a non-Newtonial fluid past an infinite porous plate, Int. J. Non-Linear Mech. 21 (1986) 279.